Available online at www.sciencedirect.com
ScienceDirect
Trans. Nonferrous Met. Soc. China 26(2016) 1745−1754
Transactions of Nonferrous Metals Society of China
www.tnmsc.cn

Microstructural characterization and dry sliding wear behavior of spark plasma sintered Cu−YSZ composites

Jafar MIRAZIMI, Parvin ABACHI, Kazem PURAZRANG

Department of Materials Science and Engineering, Sharif University of Technology, Tehran, P. O. Box 11155-9466, Iran

Received 9 August 2015; accepted 5 February 2016

Abstract: In the present study, yttria stabilized zirconia (YSZ) reinforced Cu matrix composite specimens were produced by spark plasma sintering (SPS). For comparison, pure Cu specimen was also produced in the same conditions. The effect of particles content on microstructure, relative density, electrical conductivity, and Vickers hardness was evaluated. The pin-on-disk test was also performed to determine dry sliding wear behavior of specimens under different wear conditions. After sliding wear tests, the worn surfaces were examined by field emission scanning electron microscopy (FE-SEM). Microstructural study showed satisfactory distribution of reinforcement particles in copper matrix. The relative density up to 95% was obtained for all specimens. By increasing YSZ content from 0 to 5% (volume fraction), the electrical conductivity of specimens decreased from 99.2%IACS to 65%IACS, correspondingly. The hardness of Cu−5%YSZ composite specimen was two times greater than that of pure copper. The volume loss and wear rate of pure Cu specimen were 1.48 mm^3 and 1.5×10^{-3} mm^3/m under 50 N applied load and 1000 m sliding distance. However, for composite containing 5% YSZ particles, these values dropped to 0.97 mm^3 and 0.9×10^{-3} mm^3/m, respectively. Moreover, the friction coefficient of specimens was changed from 0.6 to 0.4. The worn surface and debris observation indicate local plastic deformation and delamination as dominant wear mechanisms for pure copper, while oxidation and ploughing for composite specimen. Accordingly, it can be concluded that the Cu−YSZ composite could be a good candidate for the electrical contact applications in relays, contactors, switches and circuit breakers requiring good electrical and thermal conductivity and capability to resist wearing.

Key words: copper matrix composite; spark plasma sintering; microstructure; electrical conductivity; sliding wear

1 Introduction

Because of excellent thermal- and electrical-conductivity, high corrosion resistance and ease of fabrication, copper and copper-based materials are widely used in cables, wires, electrical contacts, and in applications requiring good electrical current conductivity [1−8]. However, pure copper suffers from low tensile strength, low hardness and poor wear resistance [1,2,5,9]. The potential solution is to strengthen copper by various methods [9]. One of the methods to improve the physical and mechanical properties as well as the wear resistance of pure copper is the addition of reinforcement particles to it, i.e., the fabrication of Cu-based composites [10−13]. It has been shown that Cu matrix composites and/or nanocomposites represent good properties such as acceptable thermal/ electrical conductivity, improved low temperature strength, and higher wear resistance than pure copper [1,12].

Hereinto, a variety of ceramic materials such as Al_2O_3, SiC, and TiB_2 have been utilized to reinforce the copper matrix. Among these, however, fine stabilized ZrO_2 ceramic particles could be a proper reinforcing material due to their high strength and stiffness, high melting temperature, and relatively good electrical property [14]. Although, noticeable studies have been performed on the fabrication and characterization of yttria stabilized zirconia (YSZ) matrix composites reinforced with other ceramic materials [15−17], the addition of ultrafine grained YSZ particles to copper matrix and its subsequent effect on the microstructure, physical and mechanical properties as well as tribological behavior of copper matrix have been notified limitedly. According to IEPURE et al [18], the electrical conductivity of Cu/ZrO_2 composites utilized in spot welding electrodes has been influenced by the producing

Corresponding author: Jafar MIRAZIMI; Tel: +98-9390400499; Fax: +98-4152372246; E-mail: jafarmirazimi@gmail.com
DOI: 10.1016/S1003-6326(16)64289-9

parameters, porosity and the ZrO_2 contents. So, the presence of 8.04% porosity has degraded the electrical conductivity of Cu−3%ZrO_2 to (30%−45%) IACS. Nevertheless, referring to other research works [19,20], a few amount of stabilized ZrO_2 particles may improve the mechanical properties as well as the wear resistance of Cu matrix. Therefore, the main idea behind this study is the producing of Cu−YSZ composites by applying a modern sintering technique.

It is well known that one of the greatest procedures for preparation of metal matrix composites is powder metallurgy [1,10,21,22]. In this method, typically, one can select a variety of mixed metallic and ceramic powders with different sizes and morphologies to produce precise, tenacious and high operational parts utilizing the variety of consolidation/sintering processes. Recently, the spark plasma sintering (SPS) consolidation technique has been used frequently for fabrication of metal matrix composites [9,23−27]. Due to the advantages of SPS process such as short processing time, improved microstructure (smaller grain size), and obtaining approximately fully dense materials at lower temperatures compared to conventional sintering methods, this technique has been known as a novel sintering method for the super-fast densification of varying nanostructured and amorphous materials as well as intermetallic compounds, ceramics, polymers, and refractory metals [26,28−30]. RITASALO et al [9,27,31] have employed the SPS technique for the consolidation of submicron sized Cu powder, Cu/Cu_2O, and Cu/Al_2O_3 composites. The relative density measurement results were up to 97% for all composites. In addition, they have observed a little grain growth for pure sub-micron copper after being densified by SPS using 50 MPa pressure and a 1 min holding time at 873 K. In another research, ZHANG et al [32] have also reported that the initial pressure of 1 MPa, holding pressure of 50 MPa, sintering temperature of 750 °C, holding time of 6 min and heating rate of 80 °C/min could be the optimized sintering parameters for the SPS of ultrafine grained copper.

Based on above research works, the present work aims to make use of SPS process as a sintering technique for producing pure copper and ultrafine grained YSZ reinforced copper matrix composites. Furthermore, in this research, the microstructural characteristics, some physical and mechanical properties as well as tribological behavior of produced composite specimens have investigated according to related ASTM standard test methods.

2 Experimental

The copper powder (99.8% purity with a particle size less than 63 μm, Merck, Germany), and 7.5% yttria stabilized zirconium oxide powder (ZrO_2−7.5Y_2O_3, Metco 6700, Sulzer Metco, USA) were used as raw materials in this study. The pure copper and YSZ powders were simply mixed in specified volume percentages (i.e., 0, 2%, 3% and 5%) using Turbula mixer (Turbula TC2, Willey Bachhofen, Switzerland) for 1 h. Before mixing, de-agglomeration of YSZ particles was performed using ultrasonic device with proper quantity of ethanol. X-ray diffraction (XRD) pattern of mixed powders was obtained using a STOE STADIP diffractometer with Cu K_α radiation (λ=0.154060 nm) in the 2θ range of 20°−80° by the step of 0.02°.

The mixture of powders was consolidated by SPS (SPS−20T−10, Easy Fashion Metal Products Trade Co., Ltd., China) apparatus. The mixed powders were initially compacted at 100 MPa and then heated with the rate of 25 °C/min to the sintering temperature of 720 °C under vacuum of 1.8 Pa. The holding time and applied pressure at sintering temperature were 5 min and 40 MPa, respectively. During the heating of specimens up to 650 °C, the applied pressure was selected as 10 MPa. The voltage and amperage of pulsed direct current were in the range of 2−3 V and 1000−2000 A. The durations of each pulse in on and off conditions were also 12 and 2 ms, correspondingly. The diameter and height of produced disk-shape specimens were 30 mm and approximately 5 mm, respectively.

The powder particles morphology and microstructure of bulk specimens were examined using field emission scanning electron microscopy (FE-SEM, Mira3-Tescan) equipped with energy dispersive X-ray spectroscopy (EDS). The microstructural characterization was carried out after etching of specimens with a mixture of 5 g $FeCl_3$ and 50 mL HCl in 100 mL distilled water solution.

The density of specimens was measured according to Archimedes principle using a Sartorius balance with an accuracy of 0.0001 g. The Vickers hardness test was conducted using a load of 30 kg with a duration loading time of 30 s. The specific electrical resistivity of specimens was determined by measuring electrical resistivity (using GW instek LCR−8110G micro ohmmeter) and specimen dimensions at room temperature. Then, the electrical conductivity of specimens was expressed as international annealed copper standard conductivity (%IACS) unit based on the ASTM B193 standard test method.

Dry sliding wear test was carried out by pin-on-disk method according to the ASTM G99 standard test method. Three different applied normal loads (20, 50 and 80 N), four sliding distances (200, 400, 600 and 1000 m), and a constant sliding velocity of 0.4 m/s were selected to evaluate tribological behavior of unreinforced copper

and composite specimens. The cylindrical pins having 5 mm in diameter and 10 mm in length were loaded against a rotating steel disk with hardness of HV 966 and average surface roughness (R_a) of 0.35 μm. After exposing of various loads and sliding distances, the mass loss of specimens was measured in an analytical balance of 0.0001 g precision and converted to volume loss values by considering the density of specimens. To investigate the wear mechanisms, the worn surfaces and debris were analyzed using FE-SEM.

3 Results and discussion

3.1 Microstructural characterization

Figure 1 shows the morphologies of used powders. Dendritic structure of electrolytic copper powders is shown in Fig. 1(a). However, YSZ particles are almost in polygonal shaped with particle size mostly less than 150 nm as seen in Fig. 1(b).

The XRD pattern of Cu−5%YSZ as mixed powders is displayed in Fig. 2. Because of the small particle size and low content of YSZ particles, the intense peak

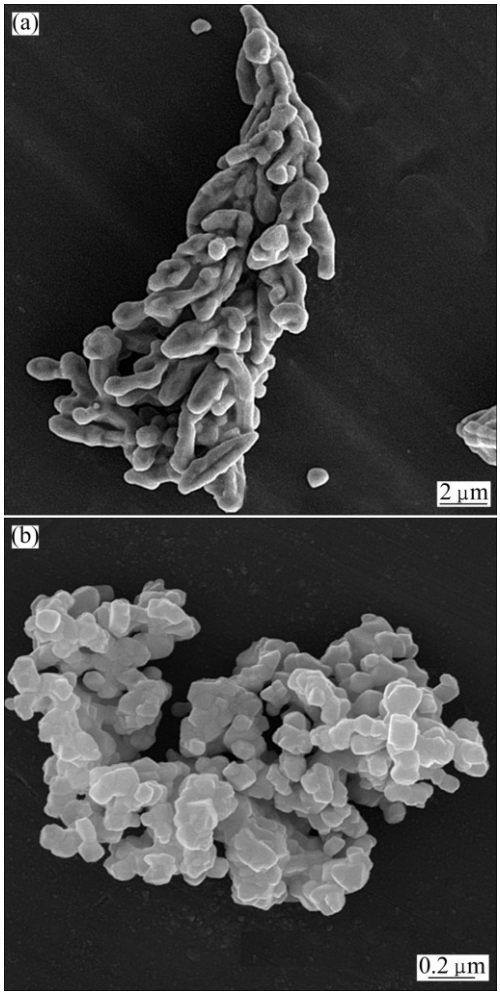

Fig. 1 Field emission scanning electron micrographs of as-received Cu (a) and milled YSZ powders (b)

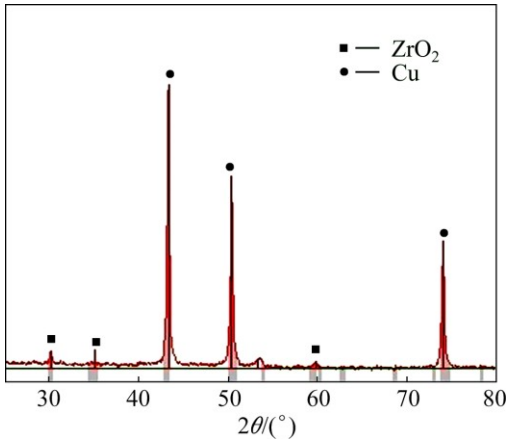

Fig. 2 XRD pattern of Cu−5%YSZ mixed powders

corresponds to Cu. According to the XRD profile and that reported by MAWSON et al [34], it is clear that zirconium oxide powder particles are tetragonally stabilized. Scherer's formula was also used for the sake of YSZ crystallite size estimation as follows:

$$D=\frac{0.9\lambda}{\beta\cos\theta} \quad (1)$$

where D is the crystallite size, λ corresponds to the X-ray wavelength (0.154060 nm in this study), β is related to the broadening of diffraction line measured as half of its maximum intensity and θ is the corresponding angle. Based on Eq. (1), the calculated crystallite size of YSZ powder equals 71 nm.

Figure 3 illustrates the microstructures of unreinforced Cu and bulk Cu matrix composites containing 2%, 3% and 5% YSZ after SPS processing. The energy dispersive spectroscopy (EDS) analysis results of two specified points in Fig. 3(b) for the Cu−2%YSZ composite are shown in Fig. 4. Figures 4(a) and (b) correspond to the EDS1 and EDS2 points which are related to the composition of YSZ particles and Cu matrix, respectively. The presence of Cu in EDS1 point could be related to great size of FE-SEM probe compared to YSZ particle diameter.

It is a well-known fact that the homogeneous distribution of reinforcement phase in the metal matrix remarkably improves the physical, mechanical, thermal properties and wear resistance of particulate reinforced metal matrix composites [10]. According to Figs. 3(b)−(d), almost uniform distribution of reinforcement particles can be seen in copper matrix. Considering the results reported by several researchers, it seems that using high energy ball milling not only has no significant effect on homogeneous distribution of (nano) particles in similar systems (for example Cu−SiC_p [35], Cu-graphite [36]) especially in those containing low content of reinforcement, but also has some incontrovertible

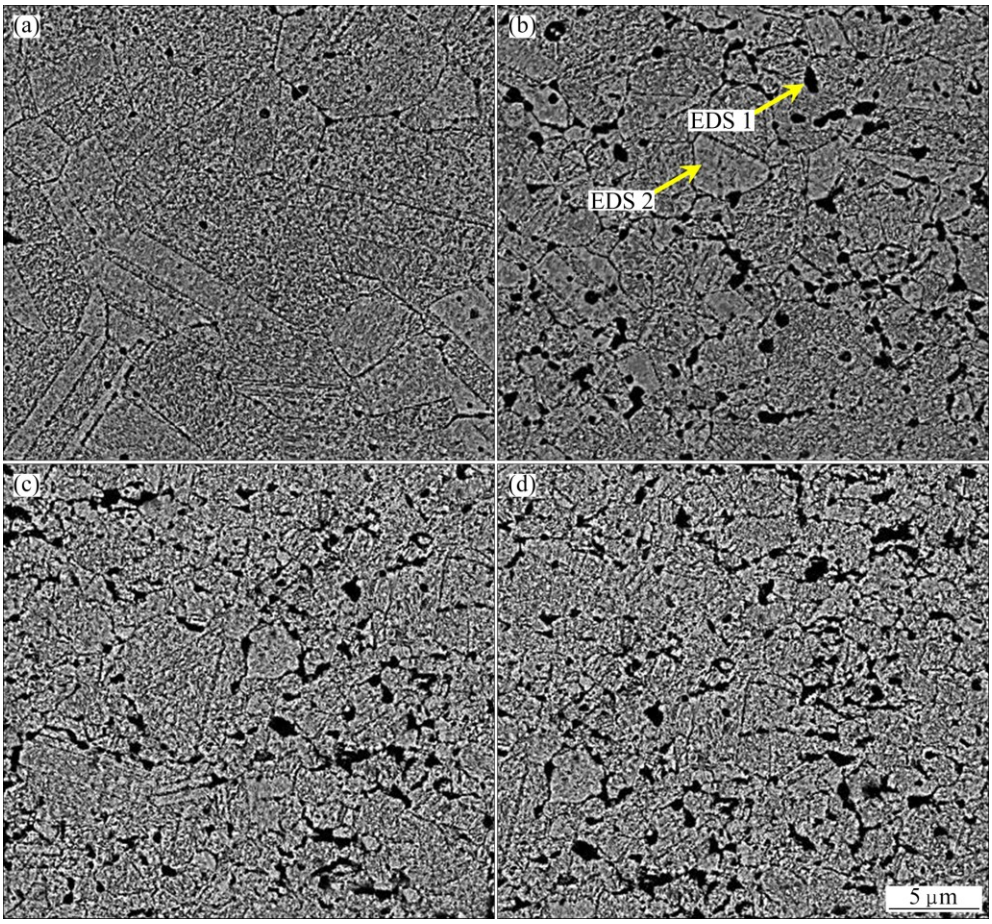

Fig. 3 Field emission scanning electron images of un-reinforced Cu (a), Cu−2%YSZ (b), Cu−3%YSZ (c), and Cu−5%YSZ (d), exhibiting distribution of YSZ particles in spark plasma sintered specimens

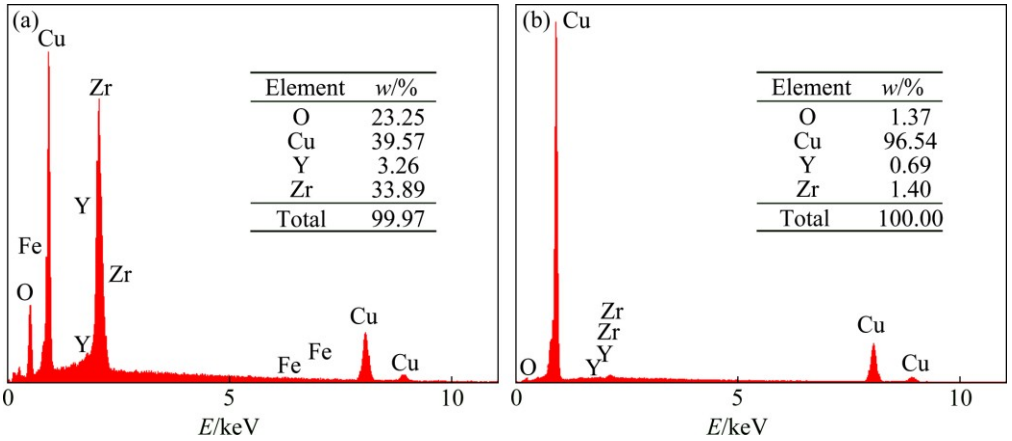

Fig. 4 EDS point analysis obtained from EDS 1 point (a) and EDS 2 point (b) in Fig. 3(b) related to composition of YSZ particles and Cu matrix, respectively

disadvantages. Therefore, in the present work, merely mixing of matrix and reinforcement powders (without any contamination) was chosen for composites processing. Another important point that can be seen in Figs. 3(a)−(d) is that by increasing of reinforcing particles content, the grain size of copper matrix decreases. The reinforcing particles could inhibit the movement of the grain boundaries and consequently grain growth.

3.2 Relative density, electrical conductivity, and hardness evaluation

The relative density, porosity, electrical conductivity and Vickers hardness values of pure copper and

composite specimens are summarized in Table 1. For determination of the theoretical density according to the rule of mixtures (ROM), the density values of copper and YSZ have been considered to be 8.96 [27] and 6.05 g/cm^3 [37], respectively. As reported by MUNIR et al [38], simultaneous applying of current and pressure as well as consideration of powders characteristics (conductive or non-conductive) during SPS as consolidation route can improve densification. As shown in Table 1, the relative density of specimens decreases with the increase in particles content. However, densification with SPS process has led to nearly full dense of specimens especially for those containing lower volume percentages of particles. It should be mentioned that, the relative density of produced composites in this work is considerably higher than those produced by conventional press−sinter and/or hot pressing consolidation processes [21,39]. DING et al [20] have investigated the relative density of Cu−ZrO_2 nanocomposites sintered by conventional method and have reported the relative density value of 72.4% for 5% YSZ reinforced Cu−ZrO_2 composite, whereas in the present study, it is higher than 95% for the same composition. However, the relative density results are comparable with those copper matrix composites consolidated via SPS technique [9,27].

Table 1 Relative density, porosity, electrical conductivity, and Vickers hardness values of Cu−YSZ composites

Material	Relative density/%	Porosity/ %	Electrical conductivity/ %IACS	Vickers hardness (HV)
Pure Cu	99.388	0.612	93.60	48.6±2.8
Cu−2%YSZ	99.205	0.795	66.90	62.9±1.35
Cu−3%YSZ	96.728	3.272	70.30	80.6±2.6
Cu−5%YSZ	95.697	4.303	61.30	107±19.06

According to Table 1, the electrical conductivity of composites is lower than that of pure copper. It should be noted that the electrical properties of a conductive material depend on this fact that how conduction electrons move in its structure. Therefore, because of the presence of reinforcement particles and/or impurities (for instance, surface impurities induced from metallography treatment) as well as the porosity as the electron scattering agents [39], the electrical conductivity of metal matrix composites reduces. However, spark plasma sintered Cu−YSZ composites in this study exhibit better electrical conductivity than those copper matrix composites which were produced by conventional sintering method [39].

The hardness of copper has been increased noticeably from HV 48.6 to HV 107 by increasing the amount of hard YSZ ceramic particles from 0 to 5%. In addition to the presence of reinforcing particles, the increment in hardness may be attributed to grain refinement and dislocations generation in the vicinity of ceramic particles as indicated by other researchers [7,40−44].

3.3 Wear test results

Figures 5(a)−(c) show the variation of volume loss with sliding distance for pure copper and composite

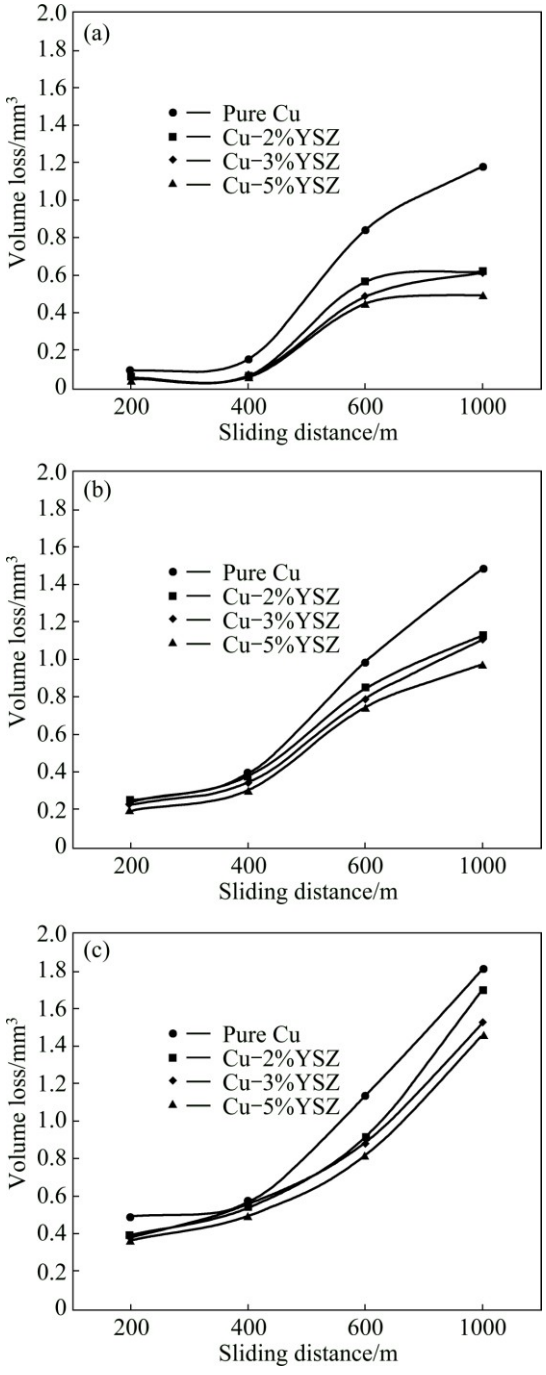

Fig. 5 Variation of volume loss with sliding distance for pure copper and composite specimens tested under three applied loads: (a) 20 N; (b) 50 N; (c) 80 N

specimens tested under three different applied loads (20, 50 and 80 N) and a constant sliding velocity of 0.4 m/s. Based on the figures, the volume loss values increase almost linearly with sliding distance for all specimens as expected [1,5,45]. However, Cu−YSZ composites, especially those containing high volume percentage of particles, have better wear resistance than pure Cu. Similar to the improvement of hardness (Table 1), it is well determined that the addition of hard ceramic particles to copper matrix contributes to the enhancement of wear resistance [12,46].

According to Fig. 6, the rise of applied load causes the considerable increase of volume loss. This could be due to the temperature rising of worn surface area between two parts (pin and stainless steel counterface) which consequently results in the higher oxidation rate and oxide removal from specimen surface as well as increasing of contact area [46,47]. However, the addition of ceramic particles can improve the resistance of composites against micro-cutting action of abrasive particles which could result in the enhancement of wear resistance, as can be seen in Fig. 6. It is well known that not only the extrinsic variables like specimen and counterface surface roughness, mechanical properties of the counterface, applied load, sliding speed, and environmental condition but also the other variables such as shape, volume fraction, size, mechanical properties and the distribution of reinforcing particles as intrinsic variables could influence the tribological behavior of metal matrix composites. Therefore, it is difficult to conclude that YSZ particles have either better wear resistance enhancement effect than other ceramic particles like SiC, TiB_2 and Al_2O_3. However, the obtained results in this work are quantitatively in good agreement with the results presented by other researchers [45].

Figure 7 shows the variation of wear rate as a function of applied load for the pure copper and composite specimens at a sliding distance of 1000 m. As expected, the wear rate of all specimens increases with an increase in the applied load. According to SHEHATA et al [21], the effect of load on the specimen is similar to the specimen indentation. By increasing the load, the penetration depth of indenter (for example hard YSZ particles) will increase, which subsequently results in high wear rate. However, Fig. 7 demonstrates that incorporation of ceramic particles contributes to the resistance of composite specimens against the penetration of abrasive particles. Similar conclusion for wear rate behavior of alumina reinforced copper matrix composites has already corroborated by FATHY et al [39]. Another point is that, according to Archad equation [46], the wear rate of composites has inverse relation with their hardness. Therefore, as can be seen in Table 1, increasing of hardness induces lower wear rate of composite specimens.

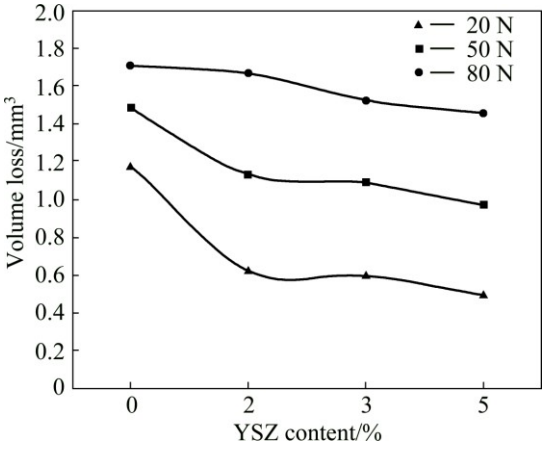

Fig. 6 Volume loss of all specimens as function of YSZ content under different applied loads and constant sliding distance of 1000 m

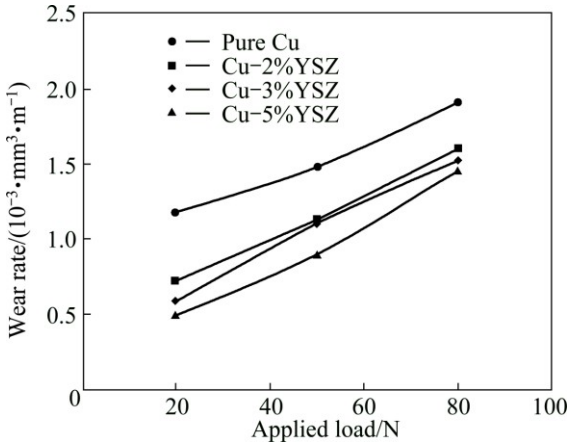

Fig. 7 Variation of wear rate as function of applied load for pure copper and composite specimens at sliding distance of 1000 m

Figures 8(a) and (b) show the variation of friction coefficient (μ) of pure Cu and Cu−5% YSZ specimens as a function of sliding distance at different applied loads. As it can be seen, almost for all applied loads, the friction coefficient increases remarkably at initial 0−200 m sliding distances and then reaches to the steady state region. The removing of asperities and surface roughness of specimen at initial sliding distances may lead to increase of two parts contact surface area and subsequently increase the friction coefficient of specimens [46]. However, decreasing of μ as a function of applied load is observed clearly in steady state region. This situation has enunciated by NATARAJAN et al [47]. The increasing of applied load can not only increase the contact surface area but also raise the temperature of two worn surfaces. It seems that the temperature rising and subsequently oxidation as well as formation and destruction of thin layer films due to applying of higher

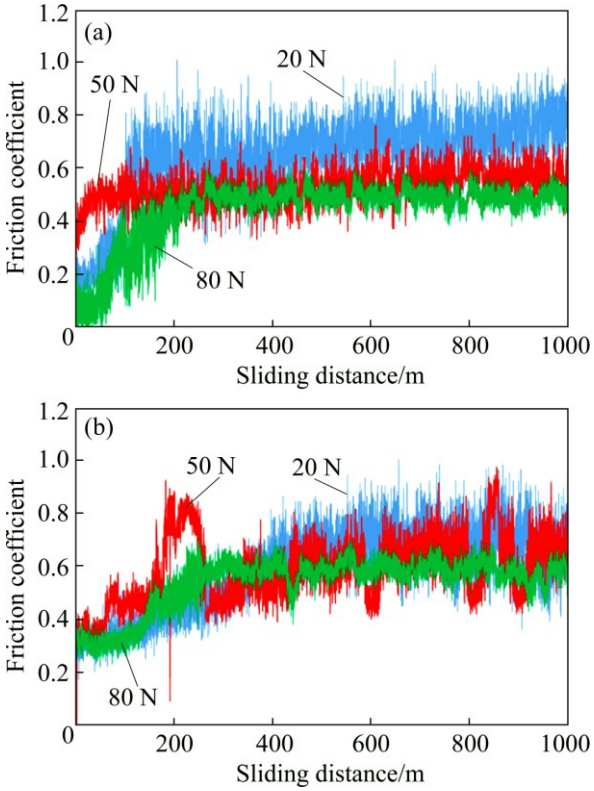

Fig. 8 Variation of friction coefficient (μ) of pure Cu (a) and Cu−5%YSZ (b) specimens as function of sliding distance at different applied loads and constant sliding velocity of 0.4 m/s

loads are the predominant factors which cause the degradation of friction coefficient in steady state region.

Figure 9 shows the average friction coefficient values of all specimens after sliding distance of 1000 m and under three different applied loads of 20, 50 and 80 N. In addition to decreasing of friction coefficient by increasing of applied load, another point which is evident in Fig. 9 is the negligible reduction of μ with the increasing of YSZ volume percentage. Inherently, harder reinforcement particles withstand the load and act as asperities and reduce the pin-counterface contact area which result in the reduction of friction coefficient [46]. For SPS consolidated coarse copper [48] and Cu/Al_2O_3 composites [11], the friction coefficient values have been reported to be 0.5−0.8 and 0.5−0.6, respectively.

In order to investigate the wear mechanisms and status of material removing, the worn surfaces of unreinforced Cu and Cu−5%YSZ composite specimens were examined using FE-SEM under different applied loads and a 1000 m sliding distance (Fig. 10). According to Fig. 10(a), under applied load of 20 N, a slight plastic deformation can be seen on the worn surface of soft copper. However, increasing of the applied load leads to some cleavage and delaminated regions (Fig. 10(b)). Surface cracking and severe material removing can also

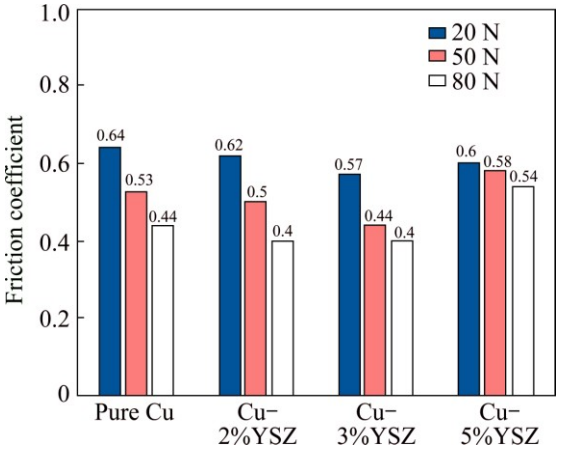

Fig. 9 Average friction coefficient values of all specimens at three different applied loads of 20, 50, and 80 N and sliding distance of 1000 m

be seen in Fig. 10(c). The plate-like debris which are shown in Fig. 11(a) confirm the occurrence of delamination and surface cracking during 80 N loading of soft copper. However, the observed phenomena on the worn surface of Cu−5%YSZ composite are slightly different with unreinforced Cu. Increasing of the applied load leads to increasing of temperature of sliding surfaces. In this condition, softening and oxidation of specimen take place. As shown in Figs. 10(d) and (e), the oxidized flakes that have remained on the worn surfaces indicate oxidation as dominant wear mechanism for composite specimen in this wear condition. Additionally, in high stress conditions (80 N applied load, Fig. 10(f)), micro-cutting and ploughing of reinforcement particles take place. Relatively coarse and coaxial debris corroborate these mechanisms occurring in copper matrix composites (Fig. 11(b)).

4 Conclusions

1) The microstructural evaluation showed that the simple mixing of powder particles and using ultrasonic device for better dispersion of reinforcement particles before mixing is a fast, easy, and low-cost method without interring any impurity and contamination to raw materials.

2) Density measurements revealed that comparing with conventional sintering methods, the SPS process is a better consolidation technique for the copper matrix composites.

3) A few amount addition of a very fine-grained and inherently hard YSZ particles to the soft copper matrix leads to considerable improvement of hardness (from HV 48 for pure copper to HV 107 for Cu−5%YSZ composite) without having significant effect on electric conductivity.

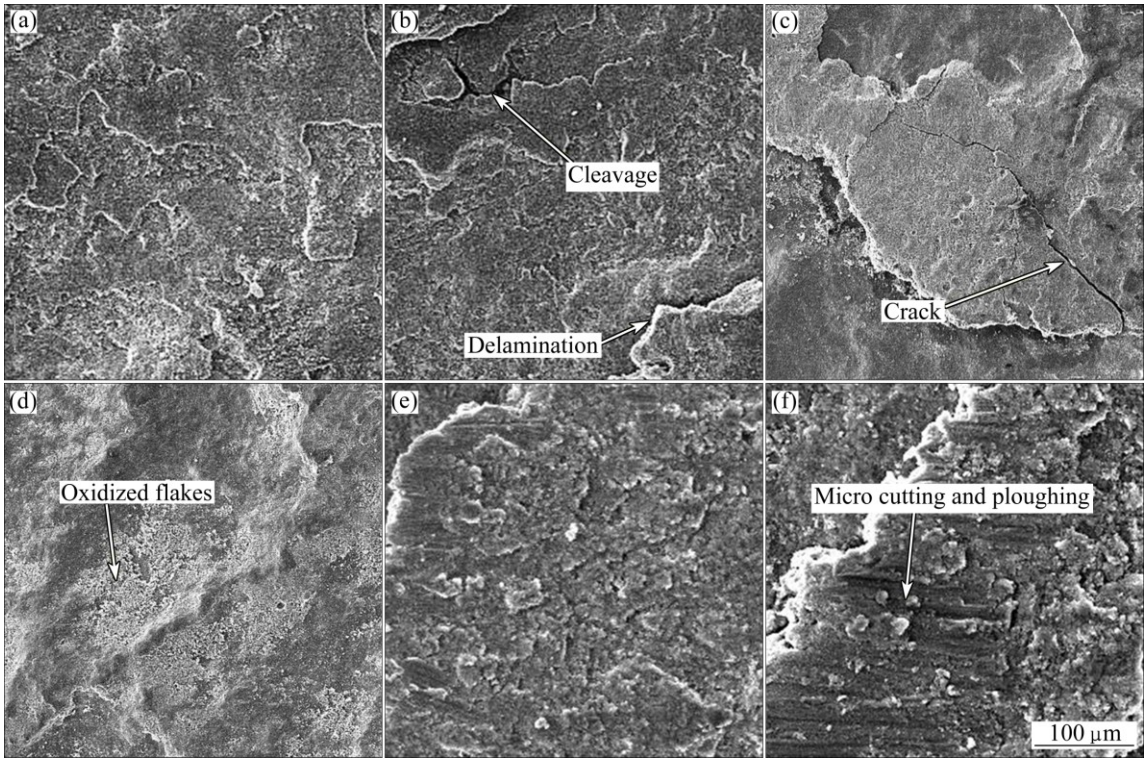

Fig. 10 FE-SEM images of worn surfaces of un-reinforced copper and Cu−5%YSZ composite at sliding distance of 1000 m and under three different applied loads: (a, b) 20 N; (c, d) 50 N; (e, f) 80 N

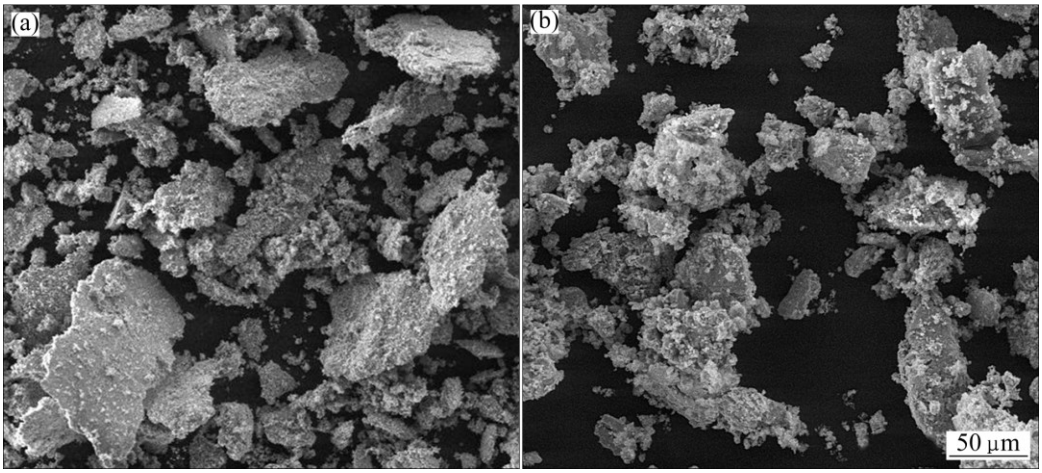

Fig. 11 FE-SEM images of collected debris of unreinforced copper (a) and Cu−5%YSZ composite specimens (b) at sliding distance of 1000 m and applied load of 80 N

4) The presence of reinforcement phase has improved the wear resistance of composite specimens effectively. An increase in particles volume fraction results in the increase of wear resistance. Small degradation of friction coefficient with increasing of applied load was observed. The worn surface and debris observations indicate local plastic deformation and delamination as dominant wear mechanisms for pure copper while oxidation and ploughing for composite specimen.

Acknowledgments

The authors wish to thank the research board of Materials and Energy Research Center of Iran (MERC) for the provision of the research facilities used in this work.

References

[1] ÇELIKYÜREK I, KORPE N O, OLCER T, GURLER R. Microstructure, properties and wear behaviors of $(Ni_3Al)_p$ reinforced

Cu matrix composites [J]. Materials Science Technology, 2011, 27: 937−943.

[2] AKHTAR F, ASKARI S J, ALI S K, DU X, GUO S. Microstructure, mechanical properties, electrical conductivity and wear behavior of high volume TiC reinforced Cu-matrix composites [J]. Materials Characterization, 2009, 60: 327−336.

[3] GIRISH B M, BASAWARAJ B R, SATISH B M, SOMASHEKAR D R. Electrical resistivity and mechanical properties of tungsten carbide reinforced copper alloy composites [J]. International Journal of Composite Materials, 2012, 2: 37−42.

[4] LARIONOVA T, KOLTSOVA T, FADIN Y, TOLOCHKO O. Friction and wear of copper–carbon nanofibers compact composites prepared by chemical vapor deposition [J]. Wear, 2014, 319: 118−122.

[5] TJONG S C, LAU K C. Tribological behaviour of SiC particle-reinforced copper matrix composites [J]. Materials Letters, 2000, 43: 274−280.

[6] ZHANG Jie, HE Ling-feng, ZHOU Yan-chun. Highly conductive and strengthened copper matrix composite reinforced by $Zr_2Al_3C_4$ particulates [J]. Scripta Materialia, 2009, 60: 976−979.

[7] CELEBI EFE G, IPEK M, ZEYTIN S, BINDAL C. An investigation of the effect of SiC particle size on Cu−SiC composites [J]. Composites Part B, 2012, 43: 1813−1822.

[8] FATHY A, EL-KADY O. Thermal expansion and thermal conductivity characteristics of Cu−Al_2O_3 nanocomposites [J]. Materials and Design, 2013, 46: 355−359.

[9] RITASALO R, LIUA X W, SODERBERG O, KESKI-HONKOLA A, PITKANEN V, HANNULA S P. The microstructural effects on the mechanical and thermal properties of pulsed electric current sintered Cu−Al_2O_3 composites [J]. Procedia Engineering, 2011, 10: 124−129.

[10] AKBARPOUR M R, SALAHI E, ALIKHANI HESARI F, SIMCHI A, KIM S H. Microstructure and compressibility of SiC nanoparticles reinforced Cu nanocomposite powders processed by high energy mechanical milling [J]. Ceramic International, 2014, 40: 951−960.

[11] ZEIN EDDINE W, MATTEAZZI P, CELIS J P. Mechanical and tribological behavior of nanostructured copper–alumina cermets obtained by pulsed electric current sintering [J]. Wear, 2013, 297: 762−773.

[12] SELVAKUMAR N, VETTIVEL S C. Thermal, electrical and wear behavior of sintered Cu−W nanocomposite [J]. Materials and Design, 2013, 46: 16−25.

[13] TU J P, WANG N Y, YANG Y Z, QI W X, LIU F, ZHANG X B, LU H M, LIU M S. Preparation and properties of TiB_2 nanoparticle reinforced copper matrix composites by in situ processing [J]. Materials Letters, 2002, 52: 448−452.

[14] YANG C L, HSIANG H I, CHEN C C. Characteristics of yttria stabilized tetragonal zirconia powder used in optical fiber connector ferrule [J]. Ceramic International, 2005, 31: 297−303.

[15] KWON N H, KIM G H, SONG H S, LEE H L. Synthesis and properties of cubic zirconia–alumina composite by mechanical alloying [J]. Materials Science and Engineering A, 2001, 299: 185−194.

[16] ÜNAL N, KERN F, OVECOGLU M L, GADOW R. Influence of WC particles on the microstructural and mechanical properties of 3mol% Y_2O_3 stabilized ZrO_2 matrix composites produced by hot pressing [J]. Journal of Europian Ceramic Society, 2011, 31: 2267−2275.

[17] ZHANG Yong-sheng, CHEN Jian-min, HU Li-tian, LIU Wei-min. Pressureless-sintering behavior of nanocrystalline ZrO_2−Y_2O_3−Al_2O_3 system [J]. Materials Letters, 2006, 60: 2302−2305.

[18] IEPURE G H, VIDA-SIMITI I, JUMATE N, CIURDAS M, HOTEA V, JUHASZ I. Effect of ZrO_2 particles upon Cu-ZrO_2 material used for the spot welding electrodes [J]. Metalurgia International, 2009, 14: 21−25.

[19] LEE S Y, KANG K H, KIM J M, HONG H S, YUN Y S, WOO S K. Fabrication and characterization of Cu/YSZ cermet high-temperature electrolysis cathode material prepared by high-energy ball-milling method: I. 900 °C-sintered [J]. Journal of Alloys and Compounds, 2008, 448: 363−367.

[20] DING Jian, ZHAO Nai-qin, SHI Chun-sheng, DU Xi-wen, LI Jia-jun. In situ formation of Cu−ZrO_2 composites by chemical routes [J]. Journal of Alloys and Compounds, 2006, 425: 390−394.

[21] SHEHATA F, FATHY A, ABDELHAMEED M, MOUSTAFA S F. Preparation and properties of Al_2O_3 nanoparticle reinforced copper matrix composites by in situ processing [J]. Materials and Design, 2009, 30: 2756−2762.

[22] MOUSTAFA S F, ABDEL-HAMID Z, ABD-ELAHI A M. Copper matrix SiC and Al_2O_3 particulate composites by powder metallurgy technique [J]. Materials Letters, 2002, 53: 244−249.

[23] LONG B D, ZUHAILAWATI H, UMEMOTO M, TODAKA Y, OTHMAN R. Effect of ethanol on the formation and properties of a Cu−NbC composite [J]. Journal of Alloys and Compounds, 2010, 503: 228−232.

[24] LI Bing-hong, LIU Ying, LI Jun, CAO Hui, HE Lin. Effect of sintering process on the microstructures and properties of in situ TiB_2−TiC reinforced steel matrix composites produced by spark plasma sintering [J]. Journal of Materials Processing Technology, 2010, 210: 91−95.

[25] YU J H, WANG C B, SHEN Q, ZHANG L M. Preparation and properties of Si_p/Al composites by spark plasma sintering [J]. Materials and Design, 2012, 41: 198−202.

[26] LEON CARLOS A, RODRIQUEZ-ORTIZ G, NANKO M, AGUILAR E A. Pulsed electric current sintering of Cu matrix composites reinforced with plain and coated alumina powders [J]. Powder Technology, 2014, 252: 1−7.

[27] RITASALO R, CURA M E, LIU X W, GE Y, KOSONEN T, KANERVA U, SODERBERG O, HANNULA S P. Microstructural and mechanical characteristics of Cu−Cu_2O composites compacted with pulsed electric current sintering and hot isostatic pressing [J]. Composites Part A, 2013, 45: 61−69.

[28] WANG Lian-jun, ZHANG Jian-feng, JIANG Wan. Recent development in reactive synthesis of nanostructured bulk materials by spark plasma sintering [J]. International Journal of Refractory Metals and Hard Materials, 2013, 39: 103−112.

[29] ZHANG Zhao-hui, LIU Zhen-feng, LU Ji-fang, SHEN Xiang-bo, WANG Fu-chi, WANG Yan-dong. The sintering mechanism in spark plasma sintering–Proof of the occurrence of spark discharge [J]. Scripta Materialia, 2014, 81: 56−59.

[30] ORRÙ R, LICHERI R, LOCCI A M, CINCOTTI A, CAO G. Consolidation/synthesis of materials by electric current activated/assisted sintering [J]. Materials Science and Engineering R, 2009, 63: 127−287.

[31] RITASALO R, CURA M E, LIU X W, SODERBERG O, RITVONEN T, HANUULA S P. Spark plasma sintering of submicron-sized Cu-powder—Influence of processing parameters and powder oxidization on microstructure and mechanical properties [J]. Materials Science and Engineering A, 2010, 527: 2733−2737.

[32] ZHANG Zhao-hui, WANG Fu-chi, WANG Lin, LI Shu-kui. Ultrafine-grained copper prepared by spark plasma sintering process [J]. Materials Science and Engineering A, 2008, 476: 201−205.

[33] REDDY K M, KUMAR N, BASU B. Innovative multi-stage spark plasma sintering to obtain strong and tough ultrafine-grained ceramics [J]. Scripta Materialia, 2010, 62: 435−438.

[34] MAWSON A G, CARTER G A, HART R D, KIRBY N M, NACHMANN A C. Mechanical properties of 8 mole% yttria-stabilised zirconia for solid oxide fuel cells [J]. Materials

Forum, 2006, 30: 148−158.
[35] AKBARPOUR M R, SALAHI E, ALIKHANI H F, KIM H S, SIMCHI A. Effect of nanoparticle content on the microstructural and mechanical properties of nano-SiC dispersed bulk ultrafine-grained Cu matrix composites [J]. Materials and Design, 2013, 52: 881−887.
[36] SAMAL C P, PARIHAR J S, CHAIRA D. The effect of milling and sintering techniques on mechanical properties of Cu-graphite metal matrix composite prepared by powder metallurgy route [J]. Journal of Alloys and Compounds, 2013, 569: 95−101.
[37] MAELAND D, SUCIU C, WAERNHUS I, HAHHMANN A C. Sintering of 4YSZ (ZrO_2 + 4 mol% Y_2O_3) nanoceramics for solid oxide fuel cells (SOFCs), their structure and ionic conductivity [J]. Journal of Europian Ceramic Society, 2009, 29: 2537−2547.
[38] MUNIR Z A, ANSELMI-TAMBURINI U, OHYANAGI M. The effect of electric field and pressure on the synthesis and consolidation of materials: A review of the spark plasma sintering method [J]. Journal of Materials Science, 2006, 41: 763−777.
[39] FATHY A, SHEHATA F, ABDELHAMEED M, ELMAHDY M. Compressive and wear resistance of nanometric alumina reinforced copper matrix composites [J]. Materials and Design, 2012, 36: 100−107.
[40] RAJKOVIC V, BOZIC D, JOVANOVIC M T. Effect of copper and Al_2O_3 particles on characteristics of Cu−Al_2O_3 composites [J]. Materials and Design, 2010, 31: 1962−1970.
[41] CHEN Ya-kun, ZHANG Xiang, LIU En-zuo, HE Chun-nian, SHI Chun-sheng, LI Jia-jun, NASH PHILIP, ZHAO Nai-qin. Fabrication of in-situ grown graphene reinforced Cu matrix composites [J]. Scientific Reports, 2016, 6: 19363.
[42] AFSHAR A, SIMCHI A. Flow stress dependence on the grain size in alumina dispersion-strengthened copper with a bimodal grain size distribution [J]. Materials Science and Engineering A, 2009, 518: 41−46.
[43] KIM Y B, LEE J, YEOM M S, SHIN J W, KIM H, CUI Y, KYSAR JEFFREY W, JAMES H, JUNG Y S, JEON S W, HAN M S. Strengthening effect of single-atomic-layer graphene in metal–graphene nanolayered composites [J]. Nature Communications, 2013: DOI: 10.1038/ncomms3114.
[44] RICHARDO C, MAURIZIO V. Metal matrix composites reinforced by nano-particles—A review [J]. Metals, 2014, 4: 65−83.
[45] GAUTMAN R K, RAY S, JAIN S C, SHARMA S. Tribological behavior of Cu−Cr−SiC_p in situ composite [J]. Wear, 2008, 265: 902−912.
[46] NEMATI N, KHOSROSHAHI R, EMAMY M, ZOLRIASATEIN A. Investigation of microstructure, hardness and wear properties of Al−4.5wt.%Cu−TiC nanocomposites produced by mechanical milling [J]. Materials and Design, 2011, 32: 3718−3729.
[47] NATARAJAN N, VIJAYARANGAN S, RAJENDRAN I. Wear behaviour of A356/25SiC_p aluminium matrix composites sliding against automobile friction material [J]. Wear, 2006, 261: 812−822.
[48] RITASALO R, ANTONOV M, VEINTHAL R, HANNULA S P. Comparison of the wear and frictional properties of Cu matrix composites prepared by pulsed electric current sintering [J]. Proceedings of the Estonian Academy of Sciences, 2014, 63: 62−74.

放电等离子烧结 Cu−YSZ 复合材料的显微组织表征和干滑动摩擦行为

Jafar MIRAZIMI, Parvin ABACHI, Kazem PURAZRANG

Department of Materials Science and Engineering, Sharif University of Technology, Tehran, P. O. Box 11155-9466, Iran

摘　要：采用放电等离子烧结制备钇稳定氧化锆(YSZ)增强铜基复合材料。为作比较，在相同条件下制备了纯铜样品。研究了粒子含量对复合材料显微组织、相对密度、电导率和维氏硬度的影响。利用销−盘装置研究材料在不同条件下的干滑动摩擦行为。干滑动摩擦测试后，采用场发射扫描电子显微镜对磨损表面进行观察。显微组织结果表明增强粒子在铜基体中分布均匀。所有样品的相对密度都达到 95%以上。当 YSZ 含量从 0 增加至 5%(体积分数)时，材料的电导率从 99.2%IACS 降至 65%IACS。Cu−5%YSZ 复合材料的硬度比纯铜硬度大两倍。在加载载荷为 50 N 和滑动距离为 1000 m 条件下，纯铜的体积损失和磨损率分别为 1.48 mm^3 和 1.5×10^{-3} mm^3/m。而对于 5% YSZ 增强的复合材料，其体积损失和磨损率分别降至 0.97 mm^3 和 0.9×10^{-3} mm^3/m。此外，材料的摩擦因数从 0.6 降至 0.4。磨损表面和磨粒观察结果表明纯铜的磨损机理为塑形变形和分层，而对于复合材料，磨损机理为氧化和犁沟。因此，Cu−YSZ 复合材料可用于要求具有高电导率和热导率以及耐磨性能的继电器、电流接触器，开关和断路器。

关键词：铜基复合材料；放电离子烧结；显微组织；电导率；滑动摩擦

(Edited by Yun-bin HE)